

# Mechanochemical Synthesis of Recyclable Biohybrid Polymer Networks Using Whole Biomass

Meng Jiang<sup>+</sup>, Emily Bird<sup>+</sup>, Woojung Ham, and Joshua C. Worch\*

**Abstract:** Whole-plant biomass from non-agricultural sources and waste biomass from processing agricultural products are both promising feedstocks for biopolymer production because they are abundant and do not compete with food production. However, their processing steps are notoriously tedious with the final materials often displaying inferior performance and limited scope in their properties. Here, we report a strategy to integrate whole-cell spirulina, a green-blue algae, into robust biohybrid algae-polyimine networks by leveraging a mechanochemical ball milling method. This strategy provides a greener synthetic approach to conventional solvent casting methods for polyimine synthesis; it simultaneously overcomes persistent constraints encountered in biomass processing and derivatization. The biohybrid algae-based materials retain adaptability and recyclability imparted by their underlying dynamic covalent polymer matrix and display enhanced mechanical properties compared to their all-synthetic equivalents. These advantageous properties are attributed to the unique morphology of the ball milled biohybrid materials which are facilitated by integration of the spirulina into the polymer matrix. Substituting spirulina with alternative biomass sources such as waste agricultural products also yields robust biohybrid networks, thus highlighting the broad utility of this straightforward mechanochemical synthesis to create more sustainable materials.

**R**enewable feedstocks are crucial to achieving a more sustainable polymer economy. Raw biomass is generally converted into functional building blocks (over multiple reaction steps), which are then used as monomers to synthesize bio-based polymers.<sup>[1–3]</sup> Alternatively, native biopolymers, such as starch and cellulose,<sup>[4,5]</sup> lignin,<sup>[6,7]</sup> or chitin<sup>[8]</sup> may be simply extracted and/or lightly functionalized to generate semi-synthetic<sup>[9]</sup> biopolymers. Despite these advances, there are persistent constraints to achieving efficient biomass processing or derivatization. Moreover, the resultant synthetic biopolymers may complicate recycling waste streams<sup>[10,11]</sup> and commonly show unpredictable environmental degradability.<sup>[12–14]</sup>

Whole (non-chemically processed) biomass from non-agricultural sources includes organisms or tissues and is another attractive feedstock for polymeric materials pro-

duction, as it introduces renewable content into materials without competing with food production.<sup>[15]</sup> Bacterial,<sup>[16,17]</sup> fungal,<sup>[18,19]</sup> and algal<sup>[20]</sup> biomass is converted into novel materials with minimal pre-processing, thus offering significant economical benefits and emission reductions compared to intensive extraction and chemical processing<sup>[21]</sup> techniques typically used for lignocellulosic biomass conversion. When surveying biomass feedstock sources, algae are particularly versatile, as they grow rapidly in non-arable lands or can be cultivated.<sup>[22,23]</sup>


Whole biomass-based materials, including those derived from algae, are typically performance-limited compared to synthetic polymers. To improve their mechanical properties, they are usually formulated into composites with added plasticizers.<sup>[24,25]</sup> A rare exception is a recent study by Roumeli and co-workers where they describe strong and stiff bioplastics obtained directly from hot pressing of whole-cell spirulina without the use of additives.<sup>[26]</sup> Nevertheless, the history of algal biomass materials predominantly focuses on blending with conventional thermoplastics, such as polyolefins or polyesters, where the algae is a filler component in the composite.<sup>[27–30]</sup> These examples typically require additional additives in combination with a reactive extrusion process to obtain materials with unsatisfactory mechanical properties. Furthermore, the complex structure of these composites likely renders it incompatible with equivalent polymer waste streams, that is, they are not recyclable, and compromises their environmental degradability.


Considering prior work with algae composites, there is interest in replacing polyolefins with alternative polymer matrices that can mitigate end-of-life concerns without compromising mechanical performance and/or requiring additives. Dynamic covalent polymer networks (DCPNs)

[\*] M. Jiang<sup>+</sup>, E. Bird<sup>+</sup>, W. Ham, J. C. Worch  
Department of Chemistry, Macromolecules Innovation Institute,  
Virginia Tech, Blacksburg, VA, USA  
E-mail: [jworch@vt.edu](mailto:jworch@vt.edu)

M. Jiang<sup>+</sup>, E. Bird<sup>+</sup>, W. Ham, J. C. Worch  
Macromolecules Innovation Institute, Virginia Tech, Blacksburg, VA,  
USA

[+] Both authors contributed equally to this work.

 Additional supporting information can be found online in the Supporting Information section

 © 2025 The Author(s). Angewandte Chemie International Edition published by Wiley-VCH GmbH. This is an open access article under the terms of the [Creative Commons Attribution-NonCommercial-NoDerivs](https://creativecommons.org/licenses/by-nc-nd/4.0/) License, which permits use and distribution in any medium, provided the original work is properly cited, the use is non-commercial and no modifications or adaptations are made.

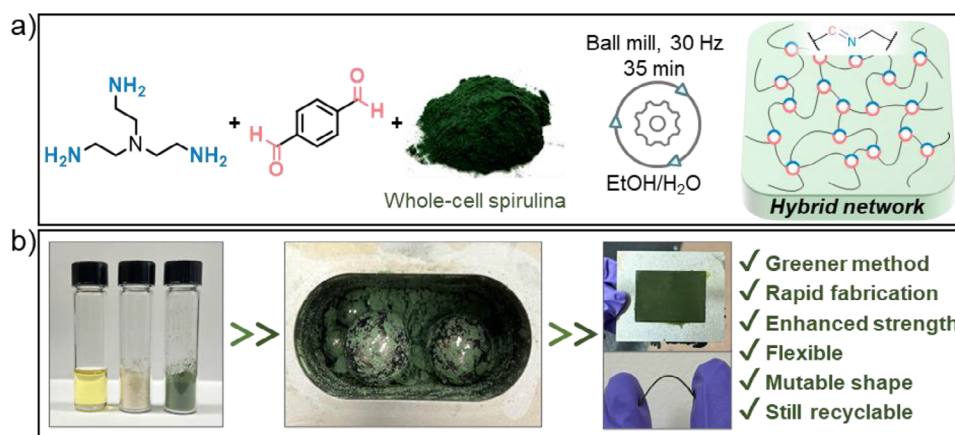


**Figure 1.** Mechanochemical synthesis of spirulina-polyimine biohybrid network using whole-cell spirulina. a) Reaction scheme showing ball milling of synthetic and biomass precursors. b) Photographs illustrating the synthetic process to produce polymer films.

are an ideal continuous polymer matrix to assess due to their mechanical likeness to high-strength thermosets in combination with thermoplastic-like recyclability owing to their transient network.<sup>[31,32]</sup> To our knowledge, there are no prior reports that use DCPNs as the matrix for algal biomass composites, nor any other whole biomass composites in general. Herein, we describe the synthesis of robust, adaptable, and recyclable biohybrid polymer networks that are formed from combining whole-cell algae (spirulina) and a dynamic polyimine network via a rapid mechanochemical synthesis (Figure 1, Scheme S1). This synthetic approach is generalizable, where other biomass sources can replace spirulina and yield strong polymeric materials.

We selected polyimine as the polymer matrix due to its straightforward fabrication, efficient recycling, and wide structure-property scope.<sup>[33–40]</sup> Spirulina was also selected as a benchmark biomass as it is economical with a high protein content and possesses a relatively weak cell wall compared to other algal biomass.<sup>[41]</sup> We hypothesized that some amino acids from the protein in spirulina would be released during processing due to its weak cell wall and serve as a complementary amino nucleophile, integrating into the polyimine network by reacting with aldehyde precursors.<sup>[42,43]</sup> Thus, this material is more accurately described as a biohybrid network rather than a conventional composite, the latter of which contains a filler and underlying polymer matrix that do not typically interact via covalent bonding. Overall, this biohybrid network structure enhances mechanical properties of the final materials since the bulk homogeneity is not significantly disrupted (*vide infra*).

We initially surveyed conventional solvent-based methods<sup>[37,40]</sup> to synthesize biomass-polyimine biohybrid networks from terephthalaldehyde (TA), tris(2-aminoethyl)amine (TREN), and whole-cell spirulina (Figure S1a–c). Although these methods were operationally simple, they required a carefully optimized solvent mixture (ethanol/water) to dissolve both the spirulina and the organic components due to their opposing solubilities. Further, the synthetic process required a multi-stage curing procedure (>1 day fabrication time), to obtain a heterogeneous film

(Figure S1d). After subsequent hot pressing of the sample, we obtained a homogeneous film (Figure S1e), but it had relatively poor mechanical properties (Figure S13).

To mitigate these synthetic challenges, we explored ball milling as a greener mechanochemical technique to fabricate biohybrid materials. Ball milling is gaining prominence in organic and polymer synthesis as it typically requires little or no solvent, delivers rapid reaction rates (compared to analogous solution-phase methods), and can even enable unique reaction pathways.<sup>[44,45]</sup> For the mechanochemical synthesis, we initially combined TA, TREN, and spirulina in a stainless steel ball mill jar (50 mL volume) equipped with stainless steel milling balls ( $2 \times \phi = 20$  mm;  $3 \times \phi = 10$  mm) and milled the sample for 35 min at 30 Hz. The milled sample appeared as a homogeneous green powder (Figure S3). However, subsequent hot pressing of the material yielded a brittle and heterogenous film with macroscopic defects (Figure S2a) and the FTIR indicated unreacted aldehyde (Figure S2b). Dry milling processes are known to depolymerize native biopolymers such as cellulose<sup>[46]</sup> or chitin,<sup>[47]</sup> which may be a contributing factor here.<sup>[48]</sup>

We then repeated the reaction (30% wt spirulina) but added a few drops of water/ethanol (1:1 v/v) to facilitate the clumping and mixing processes during milling. Liquid-assisted grinding (LAG) is known to enhance reaction conversion in some milling processes, particularly when using mainly solid substrates.<sup>[49]</sup> The LAG milling method yielded a crude sample that appeared as variable-sized flakes ( $\phi \approx 0.5$ –2 cm), distinct from the powdery samples obtained from the dry milling method (Figure S3). FTIR spectroscopy of the crude milled sample indicated near-complete conversion of the monomers as evidenced by the disappearance of the aldehyde signal ( $1685\text{ cm}^{-1}$ , C=O bond) and concomitant appearance of a new signal at  $1640\text{ cm}^{-1}$  (C=N bond) assigned to the imine species (Figure S14). The crude polymer flakes were then hot pressed using a dynamic temperature ramp (80–120 °C,  $\Delta 10\text{ °C } 5\text{ min}^{-1}$ ) to achieve a uniform film (Figures 1b, S4) suitable for assessing thermomechanical properties. The thin film showed complete conversion of monomers according to FTIR spectroscopy (Figures S14, S15). Here, the small

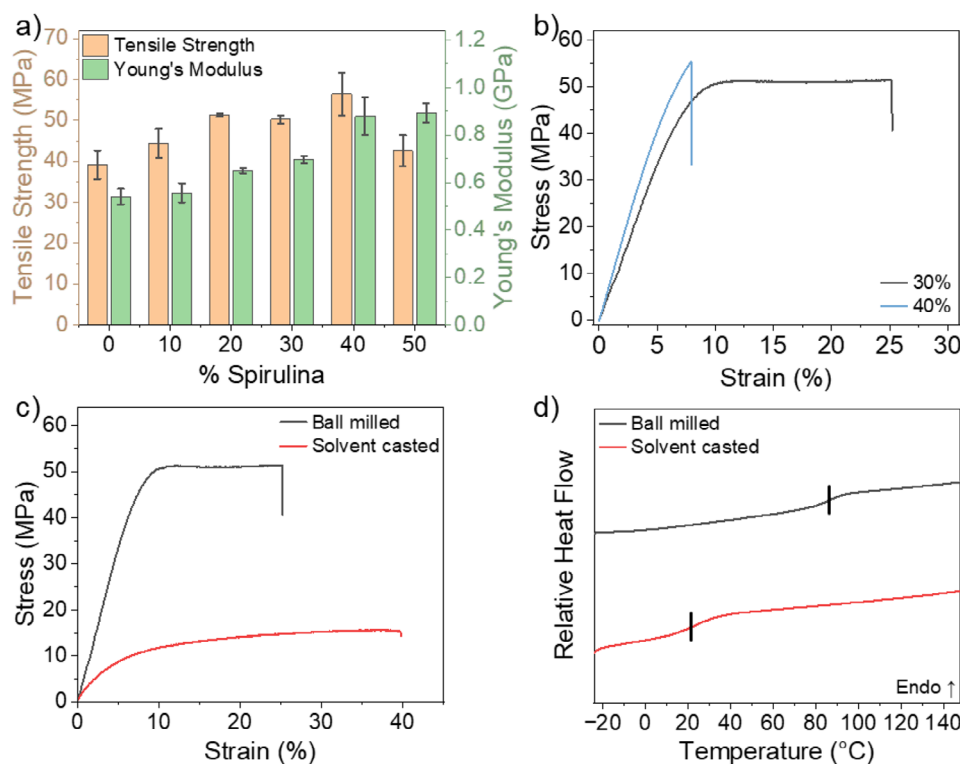


**Figure 2.** Thermomechanical properties of spirulina-polyimine biohybrid networks. a) Bar plot of tensile strength and modulus (0%–50% spirulina content) synthesized using ball mill method.  $n \geq 3$  measurements for each condition with data presented as mean  $\pm$  1 s.d. b) Representative stress versus strain curve for 30% spirulina network compared to 40% spirulina network synthesized using ball mill method. c) Representative stress versus strain curve for 30% spirulina network synthesized by ball milling or solvent casted method. d) DSC thermograms for 30% spirulina network synthesized by ball milling or solvent casted method.

amount of water present from the milling process likely also activates dynamic imine exchange when hot pressing the sample. These procedures were repeated for various formulations ranging from 0 to 60 wt% spirulina and yielded homogeneous films with complete consumption of starting monomers (Figure S15).

The thermomechanical properties of the films were assessed using uniaxial tensile testing. We observed a positive correlation between spirulina content and mechanical properties (Figures 2a, S5–S10, Table S1). In fact, the 30% spirulina sample showed a significant increase in Young's modulus (30%), tensile strength (28%), and elongation at break (92%) compared to the synthetic polyimine sample synthesized under similar conditions (Figure S8, Table S1). The 40% spirulina sample was the strongest sample of the series (Figure S9, Table S1); however, the material was brittle and broke before undergoing plastic deformation (Figure 2b). Thus, the 30% spirulina sample was chosen for further analysis. The thermal properties of the biohybrid networks were more ambiguous, where the 10% spirulina sample showed a significant reduction in glass transition temperature ( $T_g$ ) compared to the polyimine sample ( $\Delta T_g = 25$  °C) (Figures S20–S22, Table S1). However, as spirulina content increased, we observed a positive correlation with  $T_g$  according to differential scanning calorimetry (DSC) (Figures S20, S23–S27); it is possible that the spirulina has a more enhanced plasticizing effect on the network at relatively low content.<sup>[50]</sup> The 30%

spirulina sample possessed a degradation temperature ( $T_{d5\%}$ ) greater than 200 °C, which is between values obtained for samples of pure spirulina and polyimine (Figure S16).

To quantify differences between the two synthetic methods, we compared the thermomechanical properties between the solvent casted and ball milled samples at 30% spirulina content using uniaxial tensile testing and DSC. Both materials were hot pressed into thin films before thermomechanical analysis (Figure S4). We observed significant differences in their mechanical profiles, where the ball milled sample displayed a five-fold increase in Young's modulus compared to the solvent casted material (Figures 2c, S8, S11). This is likely related to their different thermal properties as the solvent casted sample possessed a lower  $T_g$  value (25 °C vs. 90 °C) (Figure 2d). Considering these results, the mechanochemical synthesis afforded materials with superior mechanical properties compared to solvent casted analogues, even for the polyimine sample (0% spirulina) (Figure S12). This suggests that ball milling methods could be more widely beneficial in the synthesis of other synthetic DCPN materials.

We then investigated the morphological differences using scanning electron microscopy (SEM) to provide insight into the enhanced bulk properties that were observed in the ball milled samples. We found nano-spherical particles in the ball milled polyimine sample (0% spirulina) (Figure 3a). This was consistent with a prior report that showed spherical features in a linear (non-network) polyimine sample synthesized from

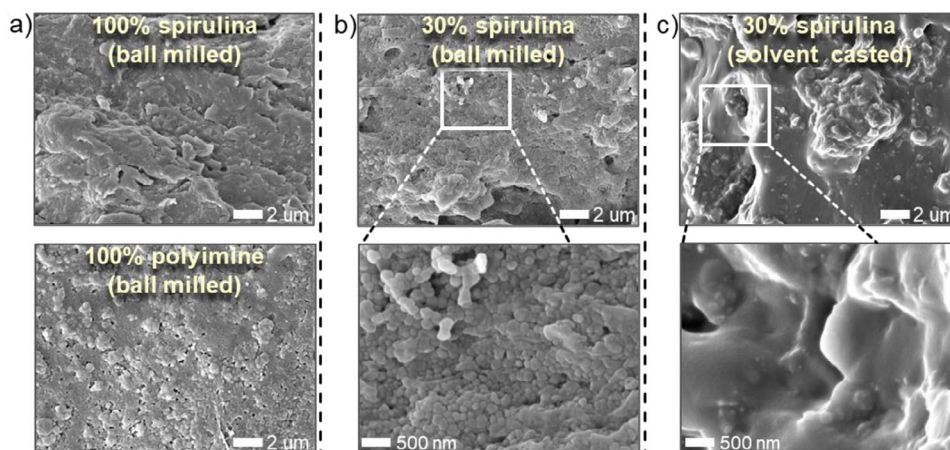


**Figure 3.** SEM micrographs of spirulina-polyimine biohybrid network films. a) Comparison of 100% spirulina sample and 0% spirulina sample (polyimine) after ball milling. b) 30% spirulina network synthesized from ball milling method. c) 30% spirulina sample synthesized from solvent casted method.

ball milling.<sup>[51]</sup> In contrast, the pure spirulina showed a heterogeneous, undefined morphology after ball milling. The 30% spirulina sample showed nano-spherical particles ( $\text{\AA} \approx 100\text{--}200$  nm), like ball milled polyimine (Figure 3b). This indicated that morphology of the polyimine was conserved, and that spirulina integrated into the bulk sample without disrupting continuity of the network. Additionally, we used SEM energy dispersive X-ray spectroscopy (SEM-EDS) to assess spirulina distribution by probing sulfur content in the materials since sulfur-containing amino acid residues in spirulina proteins would be expected to be the exclusive source of sulfur in the materials.<sup>[52]</sup> The EDS spectra showed consistent sulfur content across each sample and increased among different samples according to relative spirulina content; this indicated a homogeneous distribution of spirulina throughout the biohybrid network materials (Figures S50–S52, Table S2).

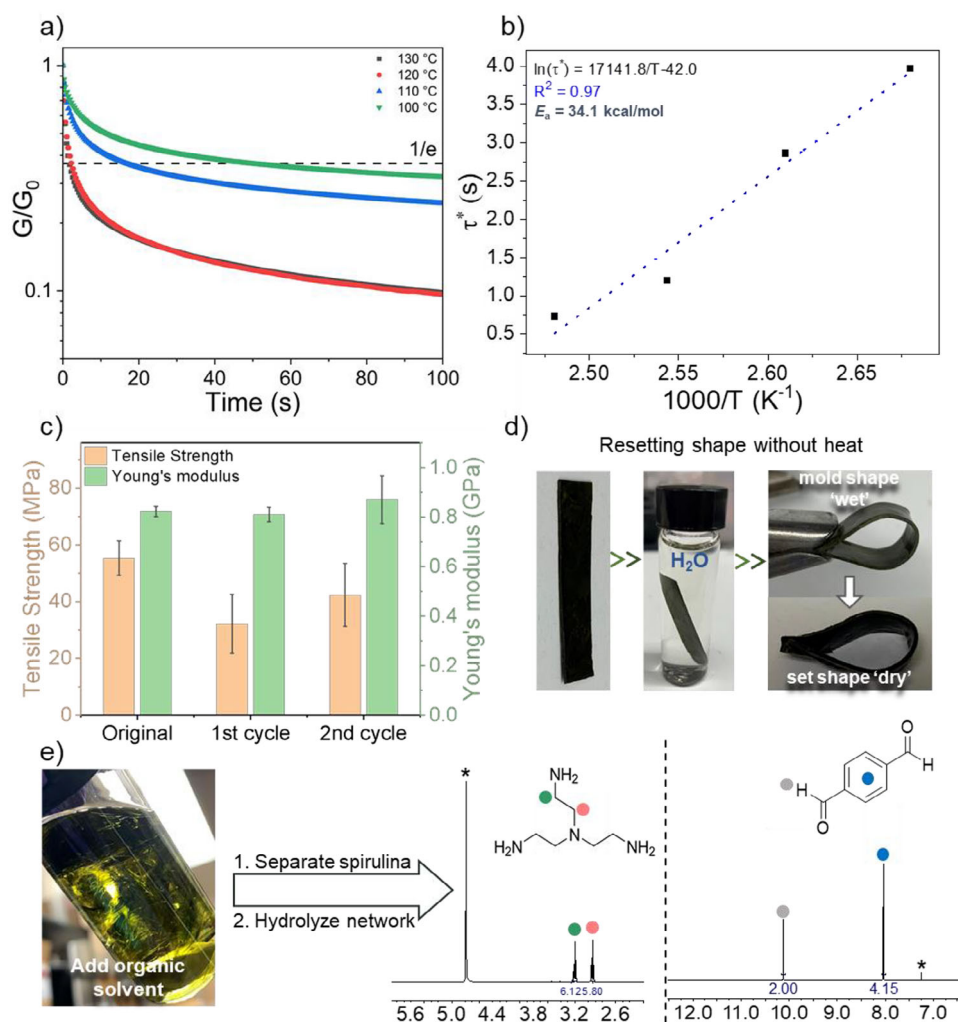
We observed similar results for the ball milled 20% spirulina sample (Figures S30, S31). However, the 30% spirulina material obtained from the conventional solvent casting method showed a heterogeneous morphology devoid of nanoscale fragments (Figure 3c). High-energy milling techniques have been historically used for particle size reduction of various materials.<sup>[53]</sup> It is reasonable to expect a similar reduction in particle sizes for spirulina and organic components alike during the ball milling process. In effect, this increases their surface area and likely promotes better interfacial contact among the particles; this enables more efficient network formation via improved accessibility of reactive sites. These morphological data corroborate the observed mechanical properties, which indicates that milling is a critical factor in obtaining materials with enhanced performance.

The information learned from bulk material properties and microscopic imaging indicates that spirulina may serve a dual role in this biohybrid material. Whole-cell spirulina is composed of approximately 60%–70% protein, 20% carbohydrates, and 6%–8% fats, among other minerals and vitamins.<sup>[54]</sup> First, in the phycocyanin protein of spirulina, amino acids with a primary amino side chain (such as lysine)

account for ca. 10%–20% of the total protein content<sup>[54]</sup>; these primary amines may participate in imine chemistry and form covalent bonding between the spirulina protein and polyimine domains (Scheme S1).<sup>[42]</sup> A control experiment using only spirulina and aldehyde without TREN showed consumption of aldehyde according to FTIR spectroscopy, suggesting imine formation between amino acid residues and aldehyde, and yielded a plastic-like film after hot pressing (Figures S43, S44).

Given the compositional complexity of this biohybrid material, we speculate on some possible explanations for the observed structure-property trends to provide further insight. The additional covalent bonding between spirulina protein and polyimine domains would likely enhance the cohesion of the hybrid network (role 1).<sup>[42]</sup> Recent work on spirulina bioplastics by Roumeli and co-workers showed that hot pressing causes protein aggregation which serves to enhance material cohesion. Likewise, other algal components such as polysaccharides, residual structured proteins, and cell wall material that remains intact after hot pressing, likely serve as additional structural reinforcements alongside protein aggregation (role 2).<sup>[55]</sup> These structural reinforcements likely contributed to the improved mechanical profiles found in polyimine-spirulina biohybrid networks as compared to the pure polyimine control. On the other hand, inert components in the whole-cell spirulina, such as carbohydrates, fats, or minerals would be expected to increase free volume within the interconnected biohybrid network matrix (role 3).<sup>[56]</sup>

At relatively low spirulina content (10%–30%), the materials are stronger and stiffer; this is likely due to synergistic effects from role 1 and 2. Additionally, role 3 could beneficially plasticize the bulk sample<sup>[50]</sup>; this would explain the lower  $T_g$  and increased ductility of the biohybrid networks compared to the polyimine sample (0% spirulina). For hybrid networks containing 40% spirulina content, the bulk material resembles a more classical composite where strength and stiffness improve while ductility decreases (Figure S9).<sup>[56]</sup> For the network with 50% spirulina content, the stiffness increased but ductility further decreased (Figure S10,



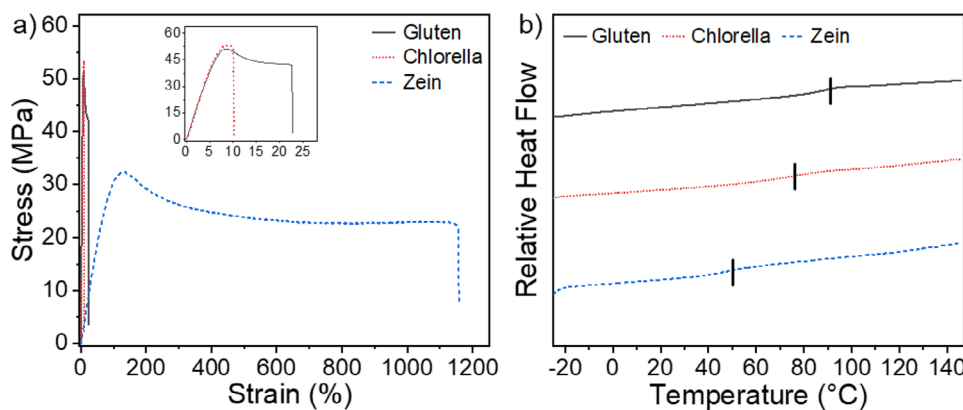
**Figure 4.** Processing and recycling of spirulina-polyimine biohybrid networks. Stress relaxation using shear oscillatory rheology at various temperatures for a) 30% spirulina sample and b) corresponding Arrhenius plot. c) Tensile strength and Young's modulus of 30% spirulina sample after repeated hot pressing,  $n \geq 3$  measurements for each condition with data presented as mean  $\pm$  1 s.d. d) Shape transformation of 30% spirulina film using water-assisted remodeling. The wet film became highly malleable and was set into a new permanent shape after subsequent drying. e) Chemical recycling or depolymerization of the network (left) and  $^1\text{H}$  NMR spectra of recovered aldehyde and amine monomers (right). \*Residual NMR solvent ( $\text{H}_2\text{O}$  and  $\text{CHCl}_3$ ).

Table S1). The 60% spirulina network was extremely brittle rendering it unsuitable for tensile analysis. As the spirulina content increases, so does the amount of non-reactive filler components; this may eventually disrupt the connectivity of the network matrix by occupying too much volume. Thus, role 3 may become detrimental at high spirulina loadings. Another explanation could be that at higher loadings these biohybrid materials simply begin to display behavior that is more characteristic of biomatter plastics (e.g., high strength and stiffness yet brittle).<sup>[26]</sup>

Next, we assessed the viscoelastic properties of the 30% spirulina sample using shear oscillatory rheology, providing insight on the adaptability and recyclability of bulk biohybrid material. Stress relaxation experiments were performed as a proxy for hot press molding. The full relaxation time is defined when the normalized relaxation modulus ( $G/G_0$ ) reaches ( $1/e$ ), or  $\sim 37\%$  of the initial stress value based on the Maxwell

model. The full-synthetic polyimine network (0% spirulina) displayed rapid relaxation kinetics with an activation energy ( $E_a = 16.2 \text{ kcal mol}^{-1}$  or  $67.8 \text{ kJ mol}^{-1}$ ) similar to previous polyimine materials.<sup>[37,40,57]</sup> Full relaxation (i.e., where the material theoretically flows for bulk remodeling) occurred in less than 5s at  $100 \text{ }^\circ\text{C}$  (Figures S47, S48). At the same temperature, the spirulina-polyimine biohybrid network relaxed approximately one order of magnitude slower ( $\approx 50 \text{ s}$ ) with  $E_a = 34.1 \text{ kcal mol}^{-1}$  or  $142.7 \text{ kJ mol}^{-1}$  (Figures 4a,b, S49). Although the relaxation kinetics are suppressed, which is expected from the addition of filler components,<sup>[58]</sup> this value still indicates adequate activation of imine bonds<sup>[59]</sup> throughout the biohybrid material and suggests it is readily moldable by hot pressing methods.

Informed by the rheology data, we assessed the recyclability of the 30% spirulina network by hot pressing the material for two additional cycles (Figures 4c, S32–S36). After



**Figure 5.** Thermomechanical properties of biomass-polyimine biohybrid networks (gluten, chlorella, or zein) synthesized using ball milling method. a) Representative stress versus strain curves for 30% biomass samples. b) DSC thermograms for 30% biomass samples.

the first recycle, the material possessed a similar stiffness ( $E = 0.81 \pm 0.02$ ) but was weaker (UTS =  $32.1 \pm 8.5$  MPa) and more brittle ( $\epsilon_{\text{break}} = 4.6 \pm 1.5\%$ ) compared to the original sample. However, we then added 10 drops of water (0.3 mL H<sub>2</sub>O for 0.7 g material) before the second pressing cycle to facilitate imine activation, and the resultant material more closely matched the original network (UTS =  $41.8 \pm 10.4$  MPa;  $\epsilon_{\text{break}} = 8.8 \pm 4.5$ ). These data indicate that the biohybrid materials retain robust properties even after remolding (Table S1).

Polyimines are known to undergo water-assisted reshaping,<sup>[40]</sup> which is analogous to heat-assisted thermoforming of thermoplastics. We conducted a similar water-reshaping experiment on the 30% spirulina biohybrid network (Figure 4d). A rectangular film was placed in water for 1 h; it was then removed and reshaped using a metal clip. While deformed in the metal clip, the sample was dried to set a new “permanent” shape. This pliability is advantageous, as it provides another simple method to reprocess the material without high heat or pressure.

Finally, if the bulk material properties deteriorated after multiple hot-press cycles, chemical recycling would serve as a complementary method to reclaim the valuable components from the material. Here, we examined the chemical recycling to monomer (CRM) of the 30% spirulina biohybrid network (Figure 4e). First, we pulverized the 30% spirulina film into a fine powder using an abbreviated ball milling process. Then, we added chloroform to solubilize the polyimine network, as previously reported by Smulders and co-workers.<sup>[60]</sup> Spirulina is mostly insoluble in organic solvents, so it was subsequently filtered and reclaimed. The reclaimed spirulina was also used to synthesize an analogous 30% biohybrid network using fresh synthetic components resulting in a material with similar strength and stiffness (Figures S45, S46). Then, the polyimine network was depolymerized by dilute HCl solution to regenerate spectroscopically pure TREN and TA components (Figures S37–S42).

We then evaluated other biomass substrates using the same ball milling method to assess the generalizability of our approach. Chlorella, gluten, and zein were substituted for spirulina to create analogous biomass-polyimine biohybrid

networks at 30% biomass content. Chlorella was chosen as a control, since it is a different algae species with a more rigid cell wall compared to spirulina and it also possesses relatively high protein content. Gluten and Zein were assessed because they are protein-rich biomass materials that are regarded as agricultural waste products.<sup>[61]</sup> Although the gluten biohybrid network was significantly more ductile than the chlorella-based material, both featured mechanical profiles that were similar to the benchmark spirulina network as evidenced by their high strength (UTS >50 MPa) and Young’s modulus (>0.8 GPa) (Figure 5a). The zein biohybrid network was comparatively soft and weaker, however the ductility was dramatically enhanced ( $\epsilon_{\text{break}} > 1100\%$ ) compared to all other samples resulting in a material with extreme toughness (Figure 5a). All were in a glassy state (testing temperature <  $T_g$ ) during mechanical analysis (Figure 5b), which makes the exceptional mechanical properties of the zein material even more remarkable. These proof-of-concept experiments reveal the broad versatility of this ball milling approach for fabricating robust biohybrid materials with tunable thermomechanical properties using diverse biomass sources.

In summary, we outline a modular and efficient mechanochemical synthesis for constructing biomass-polyimine biohybrid materials. This approach addresses prior constraints associated with synthesizing biomass-based composites. It simultaneously improves the mechanical properties of polyimine networks, especially compared to existing solution-phase methods, while mitigating waste generation. A brief survey of additional proteinaceous biomass sources using the optimized ball milling method reveals that it is broadly applicable, yielding robust materials with diverse thermomechanical properties. In future work, we plan to assess a larger range of biomass products and investigate different dynamic polymer matrices.

### Author Contributions

J.C.W. conceived the work and directed the research. J.C.W., M.J., and E.B. designed the experiments. M.J., E.B., W.H. performed and analyzed experiments. J.C.W., M.J., and E.B.

prepared the manuscript, and all authors contributed to manuscript revisions.

### Acknowledgements

The authors thank Stephen McCartney from ICTAS-NCFL for helpful discussions and assistance with SEM experiments.

J.C.W. acknowledges start-up funding from Virginia Tech and funding from 4-VA, a collaborative partnership for advancing the Commonwealth of Virginia. This work used shared facilities at the Nanoscale Characterization and Fabrication Laboratory (NCFL), which is funded and managed by Virginia Tech's Institute for Critical Technology and Applied Science (ICTAS). Additional support is provided by the Virginia Tech National Center for Earth and Environmental Nanotechnology Infrastructure (NanoEarth), a member of the National Nanotechnology Coordinated Infrastructure (NNCI), supported by NSF (ECCS 1542100 and ECCS 2025151).

### Conflict of Interests

The authors declare no conflict of interest.

### Data Availability Statement

The data that support the findings of this study are available in the Supporting Information of this article.

**Keywords:** Biomass • Dynamic covalent polymer network • Green chemistry • Mechanochemistry • Sustainability

- [1] J.-G. Rosenboom, R. Langer, G. Traverso, *Nat. Rev. Mater.* **2022**, 7, 117–137.
- [2] M. Titirici, S. G. Baird, T. D. Sparks, S. M. Yang, A. Brandt-Talbot, O. Hosseinaei, D. P. Harper, R. M. Parker, S. Vignolini, L. A. Berglund, Y. Li, H.-L. Gao, L.-B. Mao, S.-H. Yu, N. Díez, G. A. Ferrero, M. Sevilla, P. Á. Szilágyi, C. J. Stubbs, J. C. Worch, Y. Huang, C. K. Luscombe, K.-Y. Lee, H. Luo, M. J. Platts, D. Tiwari, D. Kovalevskiy, D. J. Fermin, H. Au, H. Alptekin, et al., *J. Phys. Mater.* **2022**, 5, 032001.
- [3] Y. Zhu, C. Romain, C. K. Williams, *Nature* **2016**, 540, 354–362.
- [4] F. Vilarinho, A. Sanches Silva, M. F. Vaz, J. P. Farinha, *Crit. Rev. Food Sci. Nutr.* **2018**, 58, 1526–1537.
- [5] Y. Zhang, C. Rempel, Q. Liu, *Crit. Rev. Food Sci. Nutr.* **2014**, 54, 1353–1370.
- [6] A. J. Shapiro, R. M. Dea, S. C. Li, J. C. Ajah, G. F. Bass, Epps, T. H., *Annu. Rev. Chem. Biomol. Eng.* **2023**, 14, 109–140.
- [7] R. M. O'Dea, J. A. Willie, T. H. Epps, III, *ACS Macro Lett.* **2020**, 9, 476–493.
- [8] V. Grifoll, P. Bravo, M. N. Pérez, M. Pérez-Clavijo, M. García-Castrillo, A. Larrañaga, E. Lizundia, *ACS Sustainable Chem. Eng.* **2024**, 12, 7869–7881.
- [9] Q. Xia, C. Chen, Y. Yao, J. Li, S. He, Y. Zhou, T. Li, X. Pan, Y. Yao, L. Hu, *Nat. Sustain.* **2021**, 4, 627–635.
- [10] M. J. Staplevan, A. J. Ansari, A. Ahmed, F. I. Hai, *Waste Manag.* **2024**, 185, 1–9.
- [11] S. Kakadellis, Z. M. Harris, *J. Clean. Prod.* **2020**, 274, 122831.
- [12] A. Folino, D. Pangallo, P. S. Calabrò, *J. Environ. Chem. Eng.* **2023**, 11, 109424.
- [13] E. L. Eronen-Rasimus, P. P. Näkki, H. P. Kaartokallio, *Environ. Sci. Technol.* **2022**, 56, 15760–15769.
- [14] I. E. Napper, R. C. Thompson, *Environ. Sci. Technol.* **2019**, 53, 4775–4783.
- [15] I. R. Campbell, M.-Y. Lin, H. Iyer, M. Parker, J. L. Fredricks, K. Liao, A. M. Jimenez, P. Grandgeorge, E. Roumeli, *Annu. Rev. Mater. Res.* **2023**, 53, 81–104.
- [16] A. Manjula-Basavanna, A. M. Duraj-Thatte, N. S. Joshi, *Adv. Funct. Mater.* **2021**, 31, 2010784.
- [17] A. M. Duraj-Thatte, A. Manjula-Basavanna, N.-M. D. Courchesne, G. I. Cannici, A. Sánchez-Ferrer, B. P. Frank, L. van't Hag, S. K. Cotts, D. H. Fairbrother, R. Mezzenga, N. S. Joshi, *Nat. Chem. Biol.* **2021**, 17, 732–738.
- [18] M. E. Antinori, L. Ceseracciu, G. Mancini, J. A. Heredia-Guerrero, A. Athanassiou, *ACS Appl. Bio Mater.* **2020**, 3, 1044–1051.
- [19] W. Sun, M. Tajvidi, C. G. Hunt, G. McIntyre, D. J. Gardner, *Sci. Rep.* **2019**, 9, 3766.
- [20] C. Mathiot, P. Ponge, B. Gallard, J.-F. Sassi, F. Delrue, N. L. Moigne, *Carbohydr. Polym.* **2019**, 208, 142–151.
- [21] G. Tedeschi, S. Guzman-Puyol, L. Ceseracciu, U. C. Paul, P. Picone, M. Di Carlo, A. Athanassiou, J. A. Heredia-Guerrero, *Biomacromolecules* **2020**, 21, 910–920.
- [22] V. V. Devadas, K. S. Khoo, W. Y. Chia, K. W. Chew, H. S. H. Munawaroh, M.-K. Lam, J.-W. Lim, Y.-C. Ho, K. T. Lee, P. L. Show, *Bioresour. Technol.* **2021**, 325, 124702.
- [23] W. Y. Chia, D. Y. Ying Tang, K. S. Khoo, A. N. Kay Lup, K. W. Chew, *Environ. Sci. Ecotechnol.* **2020**, 4, 100065.
- [24] J. L. Fredricks, A. M. Jimenez, P. Grandgeorge, R. Meidl, E. Law, J. Fan, E. Roumeli, *J. Polym. Sci.* **2023**, 61, 2585–2632.
- [25] C. Zhang, P.-L. Show, S.-H. Ho, *Bioresour. Technol.* **2019**, 289, 121700.
- [26] H. Iyer, P. Grandgeorge, A. M. Jimenez, I. R. Campbell, M. Parker, M. Holden, M. Venkatesh, M. Nelsen, B. Nguyen, E. Roumeli, *Adv. Funct. Mater.* **2023**, 33, 2302067.
- [27] K. Liao, P. Grandgeorge, A. M. Jimenez, B. H. Nguyen, E. Roumeli, *Sustain. Mater. Technol.* **2023**, 36, e00591.
- [28] M. A. Zeller, R. Hunt, A. Jones, S. Sharma, *J. Appl. Polym. Sci.* **2013**, 130, 3263–3275.
- [29] M. M. Hassan, M. Mueller, M. H. Wagners, *J. Appl. Polym. Sci.* **2008**, 109, 1242–1247.
- [30] T. Otsuki, F. Zhang, H. Kabeya, T. Hirotsu, *J. Appl. Polym. Sci.* **2004**, 92, 812–816.
- [31] M. Jiang, N. Mahmud, C. B. Koelbl, D. Herr, J. C. Worch, *J. Polym. Sci.* **2024**, 62, 3562–3583.
- [32] N. Zheng, Y. Xu, Q. Zhao, T. Xie, *Chem. Rev.* **2021**, 121, 1716–1745.
- [33] N. Fanjul-Mosteirín, K. Odelius, *Biomacromolecules* **2024**, 25, 2348–2357.
- [34] S. K. Schoustra, M. M. J. Smulders, *Macromol. Rapid Commun.* **2023**, 44, 2200790.
- [35] K. P. Cortés-Guzmán, A. R. Parikh, M. L. Sparacin, A. K. Remy, L. Adegoke, C. Chitrakar, M. Ecker, W. E. Voit, R. A. Smaldone, *ACS Sustainable Chem. Eng.* **2022**, 10, 13091–13099.
- [36] A. Liguori, M. Hakkarainen, *Macromol. Rapid Commun.* **2022**, 43, 2100816.
- [37] S. K. Schoustra, J. A. Dijkstra, H. Zuilhof, M. M. J. Smulders, *Chem. Sci.* **2021**, 12, 293–302.
- [38] R. Hajj, A. Duval, S. Dhers, L. Avérous, *Macromolecules* **2020**, 53, 3796–3805.

- [39] P. Taynton, C. Zhu, S. Loob, R. Shoemaker, J. Pritchard, Y. Jin, W. Zhang, *Polym. Chem.* **2016**, *7*, 7052–7056.
- [40] P. Taynton, K. Yu, R. K. Shoemaker, Y. Jin, H. J. Qi, W. Zhang, *Adv. Mater.* **2014**, *26*, 3938–3942.
- [41] L. Campanella, M. V. Russo, P. Avino, *Annales de Chimie* **2002**, *92*, 343–352.
- [42] J. Sun, H. He, K. Zhao, W. Cheng, Y. Li, P. Zhang, S. Wan, Y. Liu, M. Wang, M. Li, Z. Wei, B. Li, Y. Zhang, C. Li, Y. Sun, J. Shen, J. Li, F. Wang, C. Ma, Y. Tian, J. Su, D. Chen, C. Fan, H. Zhang, K. Liu, *Nature Commun.* **2023**, *14*, 5348.
- [43] M. B. Yim, H.-S. Yim, C. Lee, S.-O. Kang, P. B. Chock, *Ann. N. Y. Acad. Sci.* **2001**, *928*, 48–53.
- [44] A. Krusenbaum, S. Grätz, G. T. Tigineh, L. Borchardt, J. G. Kim, *Chem. Soc. Rev.* **2022**, *51*, 2873–2905.
- [45] J.-L. Do, T. Frišćić, *ACS Cent. Sci.* **2017**, *3*, 13–19.
- [46] S. M. Hick, C. Griebel, D. T. Restrepo, J. H. Truitt, E. J. Buker, C. Bylda, R. G. Blair, *Green Chem.* **2010**, *12*, 468.
- [47] H. Kobayashi, Y. Suzuki, T. Sagawa, M. Saito, A. Fukuoka, *Angew. Chem. Int. Ed.* **2023**, *62*, e202214229.
- [48] S. Amirjalayer, H. Fuchs, D. Marx, *Angew. Chem. Int. Ed.* **2019**, *58*, 5232–5235.
- [49] N. Ohn, J. Shin, S. S. Kim, J. G. Kim, *ChemSusChem* **2017**, *10*, 3529–3533.
- [50] M. L. Ampong, D. D. Catapat, D. C. Panaligan, G. M. Pantaleon, J. R. Clemeña, R. V. Rubi, F. D. Lavilles, P. J. Gildo, D. Pangayao, *IOP Conf. Ser. Mater. Sci. Eng.* **2024**, *1318*, 012019.
- [51] S. Grätz, L. Borchardt, *RSC Adv.* **2016**, *6*, 64799–64802.
- [52] A. K. Padyana, V. B. Bhat, K. M. Madyastha, K. R. Rajashankar, S. Ramakumar, *Biochem. Biophys. Res. Commun.* **2001**, *282*, 893–898.
- [53] C. F. Burmeister, A. Kwade, *Chem. Soc. Rev.* **2013**, *42*, 7660.
- [54] N. Adir, Y. Dobrovetsky, N. Lerner, *J. Mol. Biol.* **2001**, *313*, 71–81.
- [55] I. R. Campbell, Z. Dong, P. Grandgeorge, A. M. Jimenez, E. R. Rhodes, E. Lee, S. Edmundson, C. V. Subban, K. G. Sprenger, E. Roumeli, *Matter* **2025**, *8*, 101941.
- [56] Y. Li, M. L. Swartz, R. W. Phillips, B. K. Moore, T. A. Roberts, *J. Dent. Res.* **1985**, *64*, 1396–1403.
- [57] R. L. Snyder, C. A. L. Lidston, G. X. De Hoe, M. J. S. Parvulescu, M. A. Hillmyer, G. W. Coates, *Polym. Chem.* **2020**, *11*, 5346–5355.
- [58] J. D. Ferry, in *Viscoelastic properties of polymers*, John Wiley & Sons, Inc., New York, **1980**, pp. 356–357.
- [59] M. Ciaccia, S. Di Stefano, *Org. Biomol. Chem.* **2015**, *13*, 646–654.
- [60] S. K. Schoustra, V. Asadi, M. M. J. Smulders, *ACS Appl. Polym. Mater.* **2024**, *6*, 79–89.
- [61] F. De Schouwer, L. Claes, A. Vandekerckhove, J. Verduyck, D. E. De Vos, *ChemSusChem* **2019**, *12*, 1272–1303.

Manuscript received: May 13, 2025

Revised manuscript received: June 27, 2025

Accepted manuscript online: July 09, 2025

Version of record online: ■■■■■